



ELSEVIER

Available online at www.sciencedirect.com

SCIENCE @ DIRECT®

C. R. Mécanique 333 (2005) 699–705



COMPTES RENDUS

MECANIQUE

<http://france.elsevier.com/direct/CRAS2B/>

Computational AeroAcoustics: from acoustic sources modeling to farfield radiated noise prediction

Strictly stable high order difference approximations for computational aeroacoustics

Bernhard Müller*, Stefan Johansson

Division of Scientific Computing, Department of Information Technology, Uppsala University, Box 337, 751 05 Uppsala, Sweden

Available online 9 September 2005

Abstract

High order finite difference approximations with improved accuracy and stability properties have been developed for computational aeroacoustics (CAA). One of our new difference operators corresponds to Tam and Webb's DRP scheme in the interior, but is modified near the boundaries to be strictly stable. A unified formulation of the nonlinear and linearized Euler equations is used, which can be extended to the Navier–Stokes equations. The approach has been verified for 1D, 2D and axisymmetric test problems. We have simulated the sound propagation from a rocket launch before lift-off. **To cite this article: B. Müller, S. Johansson, C. R. Mécanique 333 (2005).**

© 2005 Académie des sciences. Published by Elsevier SAS. All rights reserved.

Résumé

Approximations rigoureuses stables par différences finies pour l'aéroacoustique numérique. Des schémas d'approximation par différences finies d'ordre élevé ont été développés pour l'aéroacoustique numérique dans le but d'accroître la précision et la stabilité. L'une de nos méthodes correspond au schéma de Tam et Webb, à l'intérieur du domaine, avec une modification aux limites du domaine qui permet d'obtenir une stabilité rigoureuse. Notre approche repose sur l'unification des équations non linéaires d'Euler et de leur forme linéarisée. Cette même approche pourrait être appliquée aux équations de Navier–Stokes. A titre d'exemple, la méthode est appliquée ici à des problèmes à une et deux dimensions, ainsi qu'à un problème axisymétrique. Un exemple simule l'acoustique induite par une fusée avant décollage. **Pour citer cet article : B. Müller, S. Johansson, C. R. Mécanique 333 (2005).**

© 2005 Académie des sciences. Published by Elsevier SAS. All rights reserved.

Keywords: Acoustics; Finite difference methods; High order; Aeroacoustics

Mots-clés: Acoustique; Méthodes de différences finies; D'ordre élevée; Aéroacoustique

* Corresponding author.

E-mail addresses: Bernhard.Muller@it.uu.se (B. Müller), Stefan.Johansson@it.uu.se (S. Johansson).

1. Introduction

High order finite difference methods have been developed, which are constructed to be strictly stable for linear hyperbolic and parabolic problems [1,2]. These methods satisfy the summation by parts (SBP) property, which is analogous to integration by parts and essential to obtain energy estimates. SBP operators have been applied to linear equations [3] and the nonlinear Euler and Navier–Stokes equations [4,5].

Recently, we have devised strictly stable difference methods minimizing the dispersion error [6]. In the interior, one of our new schemes corresponds to Tam and Webb’s dispersion relation preserving (DRP) scheme [7]. However, opposed to other boundary treatments in the literature, the new schemes are constructed to be stable for initial-boundary value problems and not just for periodic problems. Thus, the new schemes are well suited for CAA, where high accuracy and stability over long times are essential. Here, we apply high order SBP operators to a 1D test problem and the nonlinear axisymmetric Euler equations for sound propagation problems. The accuracy and stability of our approach applied to the nonlinear 2D Euler equations with and without entropy splitting [4,8] have been assessed by comparison with the exact solution of the sound generated by a Kirchhoff vortex, i.e. an elliptical vortex patch, cf. [9–11].

2. Euler equations

Noise propagation is modeled by the Euler equations. The perturbation formulation is used to minimize numerical cancellation errors for compressible low Mach number flow. The nonlinear conservation laws of mass, momentum and energy are expressed in terms of the changes of the conservative variables with respect to their stagnation values. Note that no approximation is made [10]. In Cartesian coordinates, the perturbed axisymmetric Euler equations can be written as

$$\mathbf{U}'_t + \mathbf{F}'_x + \mathbf{G}'_y = \mathbf{S} \quad (1)$$

where

$$\mathbf{U}' = \begin{pmatrix} \rho' \\ (\rho u)' \\ (\rho v)' \\ (\rho E)' \end{pmatrix}, \quad \mathbf{F}' = \begin{pmatrix} (\rho u)' \\ (\rho u)'u' + p' \\ (\rho v)'u' \\ (\rho H)'u' + (\rho H)_0 u' \end{pmatrix}$$

$$\mathbf{G}' = \begin{pmatrix} (\rho v)' \\ (\rho u)'v' \\ (\rho v)'v' + p' \\ (\rho H)'v' + (\rho H)_0 v' \end{pmatrix}, \quad \mathbf{S} = -\frac{1}{y} \begin{pmatrix} (\rho v)' \\ (\rho u)'v' \\ (\rho v)'v' \\ (\rho H)'v' + (\rho H)_0 v' \end{pmatrix}$$

with

$$\rho' = \rho - \rho_0, \quad (\rho \mathbf{u})' = \rho \mathbf{u}, \quad \mathbf{u}' = \frac{(\rho \mathbf{u})'}{\rho_0 + \rho'}, \quad p' = (\gamma - 1) \left[(\rho E)' - \frac{1}{2} (\rho \mathbf{u})' \cdot \mathbf{u}' \right]$$

$$(\rho E)' = \rho E - (\rho E)_0, \quad (\rho H)' = (\rho E)' + p'$$

t is time, and x and y are the axial and radial coordinates, respectively. ρ denotes the density, u and v the x - and y -direction velocities, E the specific total energy, and p the pressure. ρ_0 , $(\rho E)_0$ and $(\rho H)_0$ denote the stagnation quantities of density, total energy density and total enthalpy density, respectively. General geometries are treated by a coordinate transformation $x = x(\xi, \eta)$, $y = y(\xi, \eta)$. The transformed Euler equations in perturbation form may, for example, be found in [10].

The 2D Euler equations are obtained for $\mathbf{S} \equiv 0$ in (1). If the nonlinear terms in (1) are neglected, the linearized Euler equations are obtained. Then, $(\rho \mathbf{u})' = \rho_0 \mathbf{u}'$ and $p' = (\gamma - 1)(\rho E)'$.

The multi-dimensional applications start from silence, i.e. the initial condition $\mathbf{U}' = 0$, except for the boundary, where the sound is generated. For the rocket launch application, noise is modeled as a time harmonic velocity perturbation. Non-reflecting boundary conditions are implemented by the first approximation of the Engquist–Majda absorbing boundary conditions. Since the axis of symmetry, i.e. the x -axis, is straddled, the axisymmetric boundary conditions are imposed by symmetry of ρ' , $(\rho u)'$, $(\rho E)'$ and by anti-symmetry of $(\rho v)'$. At a solid wall, the normal velocity is set equal to zero.

3. High order method

3.1. Summation by parts (SBP) property

Assume that the computational domain $[0, 1]$ is discretized by $N + 1$ grid points $x_m = mh$, $m = 0, 1, \dots, N$, with $h = \frac{1}{N}$. High order difference operators Q for ‘d/dx’ satisfying the SBP property

$$(u, Qv)_h = u_N^T v_N - u_0^T v_0 - (Qu, v)_h \tag{2}$$

where $u, v \in \mathbb{R}^{N+1}$, can be constructed [13,2,14]. The discrete scalar product and norm are defined by

$$(u, v)_h = hu^T H v, \quad \|u\|_h^2 = (u, u)_h \tag{3}$$

where H is a symmetric positive definite $(N + 1) \times (N + 1)$ matrix. Here, H is a diagonal matrix [2]. For the rocket launch noise application, we employ a SBP satisfying difference operator Q [2] with third-order accuracy near the boundaries that coincides with the classical sixth-order central difference operator for the interior points.

The resulting ODE system is solved in time by the classical fourth-order explicit Runge–Kutta method. The metric terms are discretized by the same difference operators as the flux derivatives to maintain the order of accuracy of the scheme in curvilinear coordinates. As H is diagonal, the SBP property is kept with the metric terms. In the rocket launch noise application, the boundary conditions are imposed by injection, i.e. they are satisfied after a complete Runge–Kutta time step. This simple implementation of the boundary conditions goes at the expense of reduced stability.

Spurious high frequency oscillations are suppressed by a characteristic-based filter [9–11]. Fourth and sixth order low pass filters were found to be less accurate than the present characteristic-based filter [12].

3.2. SBP operators for DRP schemes

Dispersion Relation Preserving (DRP) schemes have attracted interest in computational aeroacoustics [7]. The formal accuracy of the method is lowered to get a better approximation of the wave number and thus a lower dispersion error. Using

$$\frac{1}{h} \sum_{j=1}^{\tau+1} \alpha_j (u_{m+j} - u_{m-j}) \tag{4}$$

as an approximation of $du(x_m)/dx$ and choosing the coefficients α_j , $j = 1, \dots, \tau + 1$, such that the accuracy becomes 2τ , the coefficients α_j will contain a free parameter. The approximate wave number \tilde{k} is given by

$$h\tilde{k} = 2 \sum_{j=1}^{\tau+1} \alpha_j \sin(jhk) \tag{5}$$

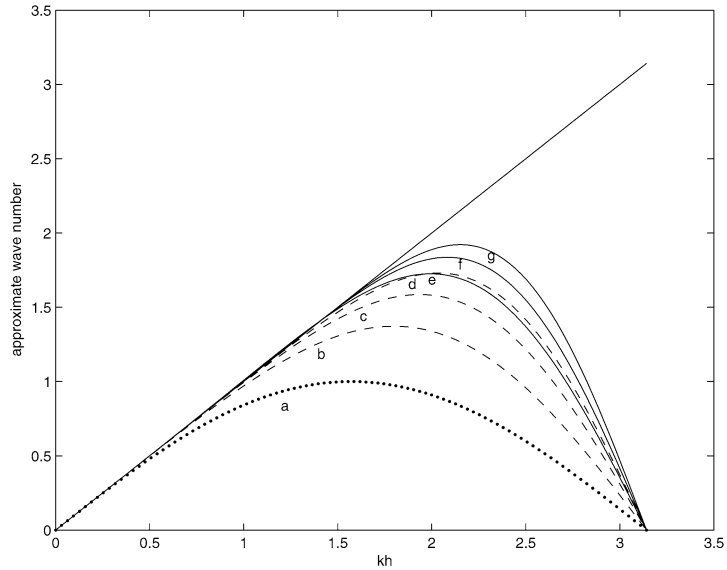


Fig. 1. Approximate nondimensional wave number $h\tilde{k}$ versus exact one hk for 2nd (a), 4th (b), 6th (c) and 8th (d) order standard centered difference methods (dashed) and DRP schemes of order four (e) six (f) and eight (g) (solid).

Fig. 1. Approximation du nombre d'onde adimensionnel $h\tilde{k}$ en comparaison de la valeur exacte hk pour les schémas centrés classiques (tirets) d'ordre 2 (a), 4 (b), 6 (c), 8 (d), et les schémas DRP d'ordre quatre (e), six (f) et huit (g) (ligne).

The free parameter is chosen such that the L_2 error squared

$$\int_{-\pi/2}^{\pi/2} |hk - h\tilde{k}|^2 d(hk) \tag{6}$$

is minimized. A comparison between standard centered finite difference methods and DRP schemes is given in Fig. 1, where $h\tilde{k} = h\tilde{k}(hk)$ is plotted. The wave number is clearly better approximated with the DRP schemes than with the standard centered difference methods.

Given a DRP scheme of order 2τ with coefficients $\alpha_j, j = 1, \dots, \tau + 1$, a difference operator Q which is accurate of order τ near the boundary and a diagonal scalar product matrix H in (3) will be derived such that the summation by parts property (2) is fulfilled. For more details see [6].

To sketch the derivation of the operator Q , we consider for simplicity the approximation of the derivative $\frac{d}{dx}$ for $x \in [0, \infty)$. The difference operator Q has to be modified for rows $1, \dots, 2\tau$. Q has the following structure [13]

$$hQ = H^{-1} \begin{pmatrix} B & C \\ -C^T & D \end{pmatrix} \tag{7}$$

where B is a full 2τ by 2τ matrix, C is a lower triangular matrix and D is an antisymmetric band matrix.

We require HQ to be antisymmetric, except for $h_{00}q_{00} = -1/2$, for Q to satisfy the SBP property. Moreover, HQ should match the DRP scheme in the interior. τ th order accuracy near the boundary requires the difference operator Q applied to polynomials of degree $0, \dots, \tau$ to yield the exact first derivatives. Then, we can express the first 2τ elements in the diagonal matrix H in terms of $\tau(2\tau - 1)$ elements of HQ . The other diagonal elements of H are 1, and the other elements of HQ and Q correspond to the DRP scheme. All these conditions lead to a system of equations to determine the $\tau(2\tau - 1)$ unknown elements of HQ . Knowing HQ and thus H, Q can be computed.

Table 1
Order of accuracy for u^I using SBP 2-4 and SBP 2-4(6) for the 1D test case at $t = 1.5$

Tableau 1
L'ordre d'approximation pour u^I avec SBP 2-4 et SBP 2-4(6) pour le cas test 1D à $t = 1,5$

# of grid points	SBP 2-4	SBP 2-4(6)
101		
202	3.0134	3.0137
401	3.0091	3.0106
801	3.0068	3.0083

4. Results

4.1. 1D test problem

The summation by parts operators for DRP schemes were tested for the hyperbolic system

$$u_t + \begin{pmatrix} 1 & 0 \\ 0 & -1 \end{pmatrix} u_x = 0, \quad u = \begin{pmatrix} u^I \\ u^{II} \end{pmatrix} \tag{8}$$

with $0 \leq x \leq 1, t \geq 0$. With the initial data $u^I(x, 0) = \sin 2\pi x, u^{II}(x, 0) = -\sin 2\pi x$, and boundary conditions $u^I(0, t) = u^{II}(0, t), u^{II}(1, t) = u^I(1, t), t \geq 0$, the exact solution is $u^I = \sin 2\pi(x - t), u^{II} = -\sin 2\pi(x + t)$.

The boundary conditions were imposed using the simultaneous approximation term (SAT) method [14]. The orders of accuracy for SBP-2-4 (SBP operator with 2nd order near boundaries and the 4th order standard scheme in interior) and SBP-2-4(6) (SBP operator with 2nd order near boundaries and the 4th order DRP scheme derived from 6th order standard scheme in interior) agree with theory, i.e. we get the expected 3rd order accuracy, cf. Table 1. For, the global order of accuracy for a finite difference scheme is one order higher than the accuracy at the boundaries, provided the order of accuracy in the interior is larger than at the boundaries [1]. A more thorough study of these new SBP operators shows that the error is about 20% lower for SBP-2-4(6) compared to SBP-2-4 [6]. Note that no filter was used here.

4.2. Rocket launch noise

The numerical method was verified for test problem 2 of category 4 in [15]: the sound field generated by an oscillating circular piston in a wall. The details are given in [16].

The problem formulation is quite similar to the test problem [16,17,12]. Under the rocket, a duct leads the exhaust jet away from the launch zone. Between the duct and the solid wall, sound can enter the computational domain. This source of sound is approximated as an oscillating piston.

The problem setting can be seen in Fig. 2 on the left. The rocket is modeled as a cylinder with the height 50 m and the radius 5 m. The nose cone is approximated by a hemisphere with the radius of the cylinder. The noise is assumed to be generated by a piston between the cylinder and a circle of radius 10 m, cf. Inlet/outlet boundary in Fig. 2 on the left. The piston velocity is given as a harmonic perturbation $u' = \varepsilon \sin(\omega t)$, where $\varepsilon = 10^{-4}$. If the filter coefficient κ is too low, high frequency oscillations caused by the discontinuity of u' at $x = 0, y = 10$ m are not damped. If κ is too large, the accuracy is degraded by too much numerical damping. A couple of frequencies have been investigated. Here, we only report 33 Hz.

The acoustic pressure contours computed with a smooth 240×240 grid are shown in Fig. 2 on the right. The acoustic pressure amplitude at the top of the hemisphere reaches 38% of the inlet value. The inlet maximum sound

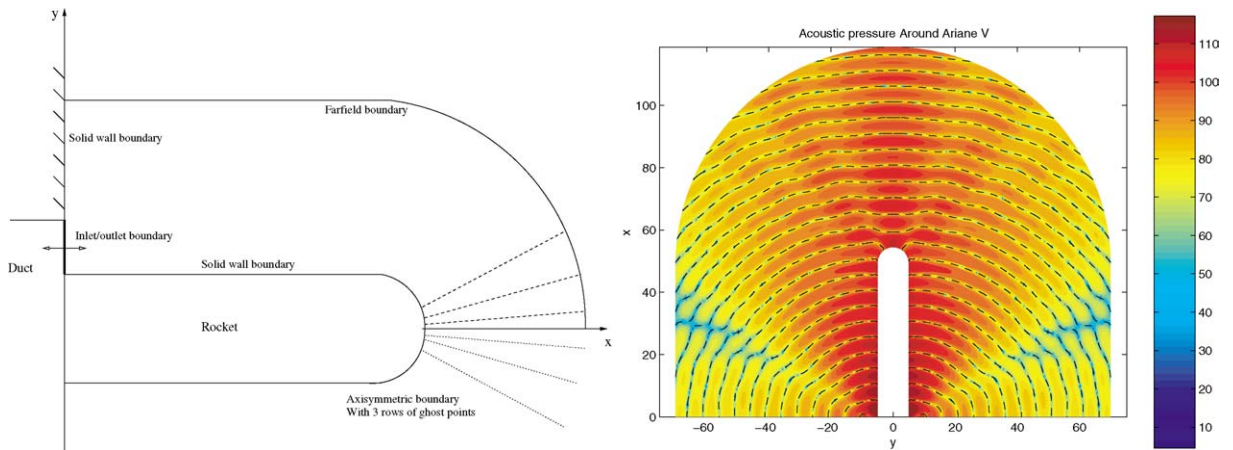


Fig. 2. Left: The source of sound is an oscillating piston that oscillates in the x -direction, cf. Inlet/outlet boundary. The axisymmetric boundary is located at $y = 0$. Right: Solution for p' when the frequency is 33 Hz. The acoustic pressure is measured in dB. The dashed lines indicate isobars where the acoustic pressure is 0.

Fig. 2. À gauche : La source acoustique est un piston oscillant dans la direction x , cf. Inlet/outlet boundary (Bord entrée/sortie). L'axe de symétrie est localisé à $y = 0$. À droite : Solution pour p' pour une fréquence de 33 Hz. La pression acoustique est mesurée en dB. Les lignes en pointillés sont les isobarres où la pression acoustique est 0. Légende : Rocket = Fusée, Solid wall boundary = Bord de paroi rigide, Duct = Canal, Inlet/outlet boundary = Bord entrée/sortie, Farfield boundary = Bord de rayonnement, Axisymmetric boundary with 3 rows of ghost points = Bord axisymétrique avec 3 lignes de points fictifs.

pressure level corresponds to 120 dB. This gives a maximum sound pressure level of 112 dB at the nose of the rocket.

5. Conclusions

We have devised strictly stable high order difference methods minimizing the dispersion error. The new schemes are constructed to be stable for initial-boundary value problems like the Euler equations. The perturbation form of the Euler equations has been discretized by a strictly stable fourth order difference method to simulate rocket launch noise propagation at low Mach numbers.

References

- [1] B. Gustafsson, H.-O. Kreiss, J. Olinger, Time Dependent Problems and Difference Methods, John Wiley & Sons, New York, 1995.
- [2] B. Strand, Summation by parts for finite difference approximations for d/dx , J. Comput. Phys. 110 (1994) 47–67.
- [3] B. Strand, Simulations of acoustic wave phenomena using high-order finite difference approximations, SIAM J. Sci. Comput. 20 (1999) 1585–1604.
- [4] M. Gerritsen, P. Olsson, Designing an efficient solution strategy for fluid flows, J. Comput. Phys. 129 (1996) 245–262.
- [5] J. Nordström, M.H. Carpenter, Boundary and interface conditions for high-order finite-difference methods applied to the Euler and Navier–Stokes equations, J. Comput. Phys. 148 (1999) 621–645.
- [6] S. Johansson, High order finite difference operators with the summation by parts property based on DRP schemes, Technical Report 2004-036, Department of Information Technology, Uppsala University, 2004. URL: <http://www.it.uu.se/research/reports/2004-036/>.
- [7] C.K.W. Tam, J.C. Webb, Dispersion-relation-preserving finite difference schemes for computational acoustics, J. Comput. Phys. 107 (1993) 262–281.
- [8] H.C. Yee, M. Vinokur, M.J. Djomehri, Entropy splitting and numerical dissipation, J. Comput. Phys. 162 (2000) 33–81.
- [9] B. Müller, H.C. Yee, High order numerical simulation of sound generation by the Kirchhoff vortex, Computing and Visualization in Science 4 (2002) 197–204.

- [10] B. Müller, High order difference method for low Mach number aeroacoustics, in: ECCOMAS Computational Fluid Dynamics Conference, Swansea, Wales, UK, 2001.
- [11] B. Müller, H.C. Yee, Entropy splitting for high order numerical simulation of vortex sound at low Mach numbers, *J. Sci. Comput.* 17 (1–4) (2002) 181–190.
- [12] B. Müller, S. Johansson, Strictly stable high order difference approximations for the Euler equations, in: Proceedings of 10th Int. Congress on Sound and Vibration, Stockholm, 2003, pp. 3883–3890.
- [13] H.-O. Kreiss, G. Scherer, Finite element and finite difference methods for hyperbolic partial differential equations, in: C. de Boor (Ed.), *Mathematical Aspects of Finite Elements in Partial Differential Equations*, Academic Press, New York, 1974, pp. 195–211.
- [14] M.H. Carpenter, D. Gottlieb, S. Abarbanel, Time-stable boundary conditions for finite-difference schemes solving hyperbolic systems: methodology and application to high-order compact schemes, *J. Comput. Phys.* 111 (1994) 220–236.
- [15] J.C. Hardin, J.R. Ristorcelli, C.K.W. Tam (Eds.), *ICASE/LaRC Workshop on Benchmark Problems in Computational Aeroacoustics (CAA)*, NASA Conference Publication 3300, 1995.
- [16] J. Westerlund, High order simulation of rocket launch noise, Master's Thesis, Uppsala University, Sweden, 2002.
- [17] B. Müller, J. Westerlund, High order numerical simulation of rocket launch noise, in: G.C. Cohen, E. Heikkola, P. Joly, P. Neittaanmäki (Eds.), *Mathematical and Numerical Aspects of Wave Propagation*, Springer-Verlag, Berlin, 2003, pp. 95–100.